Respiratory Research

RESEARCH

Open Access

Prostaglandin D_2 metabolites activate asthmatic patient-derived type 2 innate lymphoid cells and eosinophils via the DP_2 receptor

Saskia Carstensen[1†], Christina Gress[1†], Veit J. Erpenbeck[2], Shamsah D. Kazani[3], Jens M. Hohlfeld[1,4,5], David A. Sandham[3] and Meike Müller[1*]

Abstract

Background: Prostaglandin D_2 (PGD_2) signaling via prostaglandin D_2 receptor 2 (DP_2) contributes to atopic and non-atopic asthma. Inhibiting DP_2 has shown therapeutic benefit in certain subsets of asthma patients, improving eosinophilic airway inflammation. PGD_2 metabolites prolong the inflammatory response in asthmatic patients via DP_2 signaling. The role of PGD_2 metabolites on eosinophil and ILC2 activity is not fully understood.

Methods: Eosinophils and ILC2s were isolated from peripheral blood of atopic asthmatic patients. Eosinophil shape change, ILC2 migration and IL-5/IL-13 cytokine secretion were measured after stimulation with seven PGD_2 metabolites in presence or absence of the selective DP_2 antagonist fevipiprant.

Results: Selected metabolites induced eosinophil shape change with similar nanomolar potencies except for 9α,11β-PGF_2. Maximal values in forward scatter of eosinophils were comparable between metabolites. ILC2s migrated dose-dependently in the presence of selected metabolites except for 9α,11β-PGF_2 with EC_{50} values ranging from 17.4 to 91.7 nM. Compared to PGD_2, the absolute cell migration was enhanced in the presence of Δ^{12}-PGD_2, 15-deoxy-$\Delta^{12,14}$-PGD_2, PGJ_2, Δ^{12}-PGJ_2 and 15-deoxy-$\Delta^{12,14}$-PGJ_2. ILC2 cytokine production was dose dependent as well but with an average sixfold reduced potency compared to cell migration (IL-5 range 108.1 to 526.9 nM, IL-13 range: 125.2 to 788.3 nM). Compared to PGD_2, the absolute cytokine secretion was reduced in the presence of most metabolites. Fevipiprant dose-dependently inhibited eosinophil shape change, ILC2 migration and ILC2 cytokine secretion with (sub)-nanomolar potencies.

Conclusion: Prostaglandin D_2 metabolites initiate ILC2 migration and IL-5 and IL-13 cytokine secretion in a DP_2 dependent manner. Our data indicate that metabolites may be important for in vivo eosinophil activation and ILC2 migration and to a lesser extent for ILC2 cytokine secretion.

Keywords: Eosinophil shape change, Type 2 innate lymphocyte cells, Asthma, PGD_2, DP_2, CRTH2, Fevipiprant, 13,14-Dihydro-15-keto-PGD_2, PGD_2 metabolites

*Correspondence: meike.mueller@item.fraunhofer.de
†Saskia Carstensen and Christina Gress have contributed equally
[1] Department of Biomarker Analysis and Development, Clinical Airway Research, Fraunhofer Institute of Toxicology and Experimental Medicine, Hannover, Germany
Full list of author information is available at the end of the article

Background

Allergic and non-allergic asthma are closely linked to increased production of prostaglandin D_2 (PGD_2) [1–3]. The main source of PGD_2 are mast cells, which thereby orchestrate early and late immune responses of the

innate and adaptive immune system. PGD_2 primarily signals through prostaglandin D_2 receptors 1 (DP_1) and 2 (DP_2, also known as chemoattractant receptor-homologous molecule expressed on Th2 cells [CRTH2]). Activation of DP_1 is associated with increased smooth muscle relaxation, vasodilation, vascular permeability as well as reduced leukocyte chemotaxis and cytokine secretion [4, 5]. In contrast, DP_2 signaling leads to activation, chemokinesis, migration, and cytokine production of various leukocytes such as eosinophils, basophils, T cells or type 2 innate lymphoid cells (ILC2s) [6–11].

In vivo and in vitro, PGD_2 is rapidly degraded either enzymatically or spontaneously to various PGD_2 metabolites of the D, F and J series (Fig. 1) [12, 13]. The persistence of degradation products in plasma and urine may indicate a biological relevance either by preventing or prolonging in vivo receptor signaling [6, 14–16]. Enzymatic degradation of PGD_2 leads to 13,14-dihydro-15-keto-PGD_2 (DK-PGD_2) which is a highly selective DP_2 agonist [14, 15]. In plasma, PGD_2 is mainly metabolized to Δ^{12}-PGD_2 and Δ^{12}-PGJ_2 which preferably bind to DP_2 [12, 15]. Dehydration of PGD_2 and its spontaneous degradation product 9-deoxy-PGD_2 (PGJ_2) lead to formation of 15-deoxy-$\Delta^{12,14}$-PGD_2[12,17] and 15-deoxy-$\Delta^{12,14}$-PGJ_2 [7, 17, 18], respectively, which accumulate in low concentrations and as well preferably bind to DP_2 [15]. A major enzymatically derived product of the PGD_2 metabolism

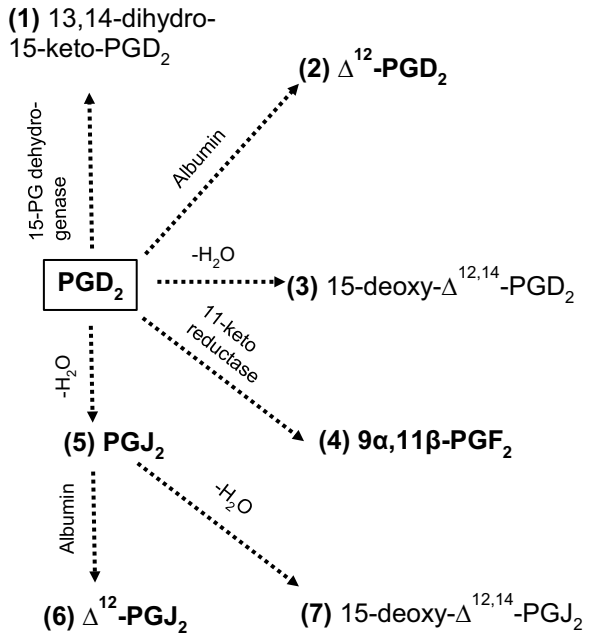

Fig. 1 Selected metabolism of prostaglandin D_2. Major metabolites are represented in bold. PGD_2, metabolite 2 and 3 belong to the D-series while metabolites 5, 6 and 7 belong to the J-series of prostaglandins. Metabolite 4 belongs to the F-series of prostaglandins

in vivo is 9α,11β-PGF_2 which is e.g. found in urine and plasma of asthmatics following allergen challenge [14, 19, 20]. Since most metabolites have selective agonistic properties for DP_2 over DP_1 they are considered to contribute to inflammatory DP_2 signaling [15, 21].

Targeting the DP_2 pathway is of significant interest for severe, uncontrolled asthmatic patients who do not or only partly respond to current available treatment options [1, 11, 22, 23]. Eosinophils and ILC2s are two major players in atopic asthma expressing DP_2. PGD_2 and metabolites activate eosinophils changing their cellular shapes [15, 18, 19], as well as inducing actin polymerization [21], CD11b expression [21] and migration [6, 12]. ILC2 numbers are increased in the airways of asthmatics and promote eosinophilia by secretion of type 2 cytokines [24, 25]. PGD_2 induces interleukin 5 (IL-5) and IL-13 secretion, cell migration, cell aggregation as well as the expression of adhesion molecules in ILC2s in a DP_2 dependent manner [26, 27]. Further, ILC2s produce endogenous PGD_2 which is degraded to PGJ_2, Δ^{12}-PGJ_2, 15-deoxy-$\Delta^{12,14}$-PGJ_2 and DK-PGD_2 in culture supernatants [28].

Fevipiprant is a potent and selective DP_2 antagonist that has shown therapeutic benefit in certain subsets of asthma patients in phase 2 clinical trials [29–31]. In a single center mechanistic phase 2 clinical trial in patients with persistent eosinophilic asthma, fevipiprant not only reduced airway inflammation, but also improved epithelial integrity and reduced airway smooth muscle mass [31, 32]. In two recently published phase 3 studies in severe asthmatics, although neither trial showed a statistically significant reduction in asthma exacerbations, consistent and modest reductions in exacerbations rates were observed in both studies with a high dose of fevipiprant [33]. In two Phase 3 studies in moderate asthmatics, no significant improvements were observed in lung function or other asthma related outcomes, such as daytime symptom score or quality of life [34]. Previously, the inhibitory effects of fevipiprant in primary human cells have been characterized with PGD_2 activation [26, 35, 36].

Here, we demonstrate the potencies of seven PGD_2 metabolites to induce ILC2 migration and IL-5 and IL-13 cytokine secretion. We also reproduce previously reported effects of the PGD_2 metabolites on eosinophil shape change. ILC2 as well as eosinophil activation was then blocked with fevipiprant demonstrating the DP_2 dependency of cell activation.

Methods

Study design

Fifteen atopic asthmatic volunteers (eight male/seven female; aged 18–65 years, average 34.5 ± 10.6 years;

BMI 19–32 kg/m^2, no oral steroids for > four weeks) were enrolled into the study. Subjects differed between eosinophil (n = 8) and ILC2 (n = 7) experiments and also between activation and inhibition experiments, respectively. Whole blood (200–500 ml) was collected in 3.8% trisodium citrate and was processed within one hour after blood withdrawal. Eosinophil levels in peripheral blood had to be > 0.15×10^6/ml for the eosinophil shape change.

Reagents

PGD_2, 13,14-dihydro-15-keto-PGD_2, PGJ_2, Δ^{12}-PGJ_2, Δ^{12}-PGD_2, 15-deoxy-$\Delta^{12,14}$-PGJ_2, 15-deoxy-$\Delta^{12,14}$-PGD_2, 9α,11β-PGF_2 were purchased from Cayman Chemicals (Biomol GmBH, Hamburg, Germany). Fevipiprant (GST0000013789) was provided by Novartis Pharma AG (Basel, Switzerland). Reagents were dissolved in sterile-filtered Hybri-Max dimethylsulfoxide (DMSO, Sigma-Aldrich, Taufkirchen, Germany).

Granulocyte isolation

Blood was stored on ice until processing. Granulocytes were isolated as described [18, 37]. In brief, 200 ml blood was diluted 1:3 in Dulbecco's Phosphate Buffered Saline (DPBS). The blood suspension was incubated with 4% (w/v) dextran-T500 (dilution 5:1, VWR, Hannover, Germany) for 30 min on ice. The upper phase was layered on Ficoll-Paque® (Sigma-Aldrich, Taufkirchen, Germany) and centrifuged (25 min, 300×*g*, 18 °C). Granulocyte pellets each were resuspended in 500 µl DPBS and erythrocytes were lysed for 40 s with 20 ml ice cold, sterile, endotoxin-free distilled water. The reaction was stopped with 20 ml DPBS (2 × concentrated). After centrifugation (10 min, 300×*g*, 18 °C), cell pellets were washed with 50 ml DPBS. Granulocytes were resuspended in assay buffer (0.1% bovine serum albumin (BSA) in DPBS, Sigma-Aldrich, Taufkirchen, Germany) to a cell density of 6.25×10^6/ml.

Eosinophil shape change

Granulocytes (80 µl) and assay buffer (10 µl) were incubated in a water bath (5 min, 37 °C). Metabolite solutions (10 µl, final concentration (conc.) 0.01 nM, 0.1 nM, 0.5 nM, 1 nM, 5 nM, 10 nM, 100 nM, 1 µM, 1% DMSO in assay buffer) were added (5 min, 37 °C). The incubation was stopped with 250 µl of 0.25% BD Cell-Fix™ Solution (1:10 with sterile water followed by 1:4 with assay buffer, BD Biosciences, Heidelberg, Germany) and immediate placement on ice (≥ 5 min). Flow cytometric analysis was performed with a Navios 3/10 (Beckman Coulter). Granulocytes were determined by FSC and SSC properties. Eosinophils were discriminated from neutrophils by autofluorescence properties at 560 nm (FL2). 1000 eosinophils were acquired. Eosinophil shape change was calculated as percentage increase of the mean FSC units.

For DP_2 inhibition experiments, granulocytes (80 µl) and fevipiprant (10 µl, final conc. 0.01 nM, 0.05 nM, 0.1 nM, 1 nM, 5 nM, 10 nM, 100 nM, 500 nM, 1 µM, 10 µM) were incubated in a water bath (5 min, 37 °C). Metabolite solution (10 µl, EC_{70} concentration) was added for 5 min (37 °C). The reaction was stopped and cells were analyzed as described above.

Type 2 innate lymphoid cell isolation

Blood was stored at RT until processing. Whole blood (500 ml) was diluted 1:2 in DPBS. PBMCs were isolated using Ficoll-Paque® and SepMate-50 PBMC Isolation tubes (STEMCELL Technologies, Grenoble, France) following manufacturer's protocol. PBMCs were pooled, washed with 50 ml DPBS and centrifuged (5 min, 300×*g*, 4 °C). T cells, B cells and monocytes depletion enriched ILC2s using CD3, CD14 and CD19 MACS separation beads (Miltenyi Biotech, Bergisch Gladbach, Germany) and LD columns following manufacturer's protocol. Enriched cells were centrifuged (5 min, 300×*g*, 4 °C) and resuspended in staining buffer containing 5% fetal bovine serum (FBS) and 2 mM ethylenediaminetetraacetic acid (EDTA) in DPBS. Cells were stained for 15 min at RT with a PerCP-Cy5.5-labeled lineage cocktail (CD4, CD8, CD14, CD16, CD19, CD34, CD123, FcεRI), CD11b-FITC, CD56-FITC, CD3-BV510, CD127-BV421, CD45-Alexa Fluor 700 and CD294-PE. View supplement for more detailed information. CD45+, Lineage-, CD11b-, CD56-, CD3-, CD127+, CD294+ cells were sorted with an FACS ARIA Fusion (BD Bioscience) into 96 U bottom well plates (Corning, Amsterdam, Netherlands).

Type 2 innate lymphoid cell culture

Sorted ILC2s (100 cells/well) were expanded with human feeder PBMCs (100,000/well; 37 °C, 5% CO_2) for three to five weeks. Culture medium contained RPMI 1640 Glutamax medium (Life Technologies, Darmstadt, Germany), 1% Pen/Strep (Life Technologies, Darmstadt, Germany), 10% *h.i.* human AB serum (Sigma-Aldrich, Taufkirchen, Germany), and 25 mM 4-(2-hydroxyethyl)-1-piperazineethanesulfonic acid (HEPES, Lonza, Wakersville, USA). The medium was supplemented with 100 U/ml rh-IL-2 (Life Technologies, Darmstadt, Germany), 25 ng/ml rh-IL-4 (Miltenyi Biotech, Bergisch Gladbach, Germany), 5 µg/ml phytohemagglutinin-M (PHA-M; Sigma-Aldrich, Taufkirchen, Germany).

Cell migration assay

Migration was assessed using 5.0 µm pore size, polycarbonate membrane, polystyrene 96-transwell plates (Corning, Amsterdam, Netherlands; Hölzel, Köln,

Germany) following manufacturer's protocols. Metabolites (lower well, final conc. 5 nM, 10 nM, 50 nM, 100 nM, 500 nM, 1 µM, 2 µM, 3 µM and 5 µM) and cells (upper well, ≤ 100,000/well) were incubated for 6 h (37 °C, 5% CO_2) in culture medium without IL-2, IL-4 and PHA. Migrated cells (25 µl) were incubated with CellTiter-Glo® Luminescence Cell Viability Assay (Promega, Mannheim, Germany) following manufacturer's protocol. Luminescence was measured using a Tecan infinite F200 pro.

For DP_2 inhibition experiments, ILC2s were incubated with fevipiprant (final conc. 0.01 nM, 0.1 nM, 0.5 nM, 1 nM, 5 nM, 10 nM, 100 nM, 1 µM, 10 µM, for 1 h, 37 °C, 5% CO_2) in culture medium without IL-2, IL-4 and PHA and cell migration was measured as described above using the EC_{70} concentration of respective metabolites.

Cytokine measurement

Cells (≤ 150,000/well) and metabolite solutions (final conc. 2.5 nM, 5 nM, 25 nM, 50 nM, 250 nM, 500 nM, 1 µM, 1.5 µM, 2.5 µM) were incubated for 24 h in culture medium without IL-2, IL-4 and PHA (U-bottom 96-well plates, 37 °C, 5% CO_2). After centrifugation (5 min, 300×*g*, RT), the supernatant was collected and stored at − 80 °C until measurement.

For DP_2 inhibition experiments, ILC2s were incubated with fevipiprant (final conc. 0.01 nM, 0.1 nM, 0.5 nM, 1 nM, 5 nM, 10 nM, 50 nM, 100 nM, 1 µM) for 1 h (37 °C, 5% CO_2) and afterwards with the EC_{70} concentration of respective metabolites for 24 h. Cells were incubated as described above.

Supernatants were diluted 1:10 and IL-5 and IL-13 concentrations were measured by MSD immunoassays (V-PLEX Meso Dale Discovery, Rockville, MD, USA) following manufacturer's protocol. Raw values are depicted in Additional file 1: Figs. S2 and S3.

Statistics

GraphPad Prism 9.0.1 was used for analysis. Four parameter non-linear agonist or inhibitor regression models were used fit curves and to calculate EC_{50}/IC_{50} values, respectively. Fitting curves constraints are indicated in respective figure legends.

Maximal PGD_2-induced responses were compared with respective maximal responses of metabolites using paired One-Way ANOVA with post-hoc Dunn's multiple comparisons tests.

Results

PGD_2 metabolites induce eosinophil shape change with similar potencies

PGD_2 and seven PGD_2 metabolites were evaluated for their ability to induce activation of eosinophils by measurement of cellular shape changes. All prostaglandins induced a concentration dependent shape change with nanomolar potency except for 9α,11β-PGF_2 which was less potent (Additional file 1: Fig. S1). EC_{50} values of prostaglandins, described as mean ± standard error of the mean (SEM), fell into following rank order: PGD_2: 0.7 ± 0.2 nM < Δ^{12}-PGD_2: 1.2 ± 1.8 nM < 15-deoxy-$\Delta^{12,14}$-PGD_2: 1.5 ± 1.6 nM < PGJ_2: 1.6 ± 3.8 nM < DK-PGD_2: 2.7 ± 2.3 nM < Δ^{12}-PGJ_2: 5.6 ± 1.0 nM < 15-deoxy-$\Delta^{12,14}$-PGJ_2: 12.0 ± 0.7 nM < 9α,11β-PGF_2: > 1000. Similar EC_{50} values were reported by Sandig et al. but with different rank order (Table 1) [19].

Table 1 EC_{50} values of PG-induced eosinophil shape change were calculated and are given as mean ± standard error of the mean (SEM), n = 2–3

Eosinophil shape change EC_{50} [nM]		
Metabolite	**Measured values**	**Sandig et al. [19]**
PGD_2	0.7 ± 0.2	0.4
DK-PGD_2	2.7 ± 2.3	1.1
Δ^{12}-PGD_2	1.2 ± 1.8	7.3
15-deoxy-$\Delta^{12,14}$-PGD_2	1.5 ± 1.6	2.4
9α,11β-PGF_2	> 1000	156.0
PGJ_2	1.6 ± 3.8	2.2
Δ^{12}-PGJ_2	5.6 ± 1.0	3.7
15-deoxy-$\Delta^{12,14}$-PGJ_2	12.0 ± 0.7	8.4

Published reference values are given in the right column

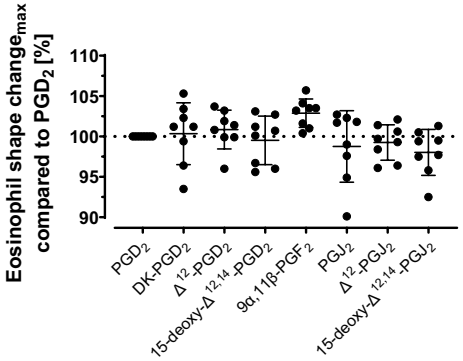

Fig. 2 Comparison of maximal eosinophil shape change in the presence of PGD_2 and selected metabolites. The mean forward scatter values in the presence of the highest PGD_2 concentration was normalized to 100% shape change, n = 6–8. Values are given as mean ± SD

Metabolites induced shape changes with similar maximal responses as compared to PGD_2, which was observed by a comparison of FSC_{max} values normalized on 100% PGD_2 shape change. Activation responses of PGD_2 metabolites ranged between 98.0 and 102.9%, compared to the parent PGD_2 (Fig. 2). Sandig et al. did not compare maximal responses but their results indicate similar

responses for most metabolites as well while responses of Δ^{12}-PGD_2 and Δ^{12}-PGJ_2 seemed to have higher FCS values.

PGD_2 metabolites induce ILC2 migration and IL-5 and IL-13 cytokine secretion

Next, PGD_2 metabolites were evaluated for their potential to induce ILC2 migration and Type 2 cytokine secretion. The metabolites induced cell migration concentration dependently and with nanomolar potency except for 9α,11β-PGF_2. 9α,11β-PGF_2 increased migration in comparison to the medium control but dose independently (Fig. 3A). Migratory potencies were increased for the D-series of metabolites in comparison to the J-series with mean $EC_{50} \pm$ SEM values of PGD_2 17.4 ± 3.9 nM, DK-PGD_2 14.2 ± 3.4 nM, Δ^{12}-PGD_2 19.3 ± 3.2 nM, 15-deoxy-$\Delta^{12,14}$-PGD_2 21.8 ± 6.3 nM, PGJ_2 66.3 ± 7.0 nM, Δ^{12}-PGJ_2 91.7 ± 9.2 nM and 15-deoxy-$\Delta^{12,14}$-PGJ_2 38.1 ± 5.4 nM (Table 2). Micromolar metabolite concentrations abolished cell migration.

The maximal migration response measured by total number of migrated cells compared to PGD_2 was increased for Δ^{12}-PGD_2, 15-deoxy-$\Delta^{12,14}$-PGD_2, PGJ_2, Δ^{12}-PGJ_2 and 15-deoxy-$\Delta^{12,14}$-PGJ_2. In contrast DK-PGD_2 and 9α,11β-PGF_2 showed a non-significant trend to reduced maximal migration responses, (Fig. 3B).

IL-5 and IL-13 cytokine secretion of ILC2s was induced by PGD_2 metabolites in a concentration dependent manner. ILC2 responses were comparable between IL-5 and IL-13 (Fig. 4A). Similar to cell migration, higher potencies for cytokine secretion were found for the D-series of metabolites compared to the J-series (Table 2). 9α,11β-PGF_2 was able to induce cytokine secretion although less potent than the other metabolites and with high variability. The maximal cytokine secretion response was significantly lower in the presence of 9α,11β-PGF_2 and PGJ_2 compared to PGD_2 while the maximal response was similar for DK-PGD_2, Δ^{12}-PGJ_2 and 15-deoxy-$\Delta^{12,14}$-PGJ_2. Cytokine secretion was non-significantly enhanced for Δ^{12}-PGD_2 and 15-deoxy-$\Delta^{12,14}$-PGD_2 compared to PGD_2 (Fig. 4B).

Selective DP_2 inhibition of eosinophils and ILC2s

Isolated whole blood eosinophils were incubated with the selective DP_2 antagonist fevipiprant prior to activation of cells with EC_{70} concentrations of PGD_2 or respective metabolites (supplementary table 2). Fevipiprant inhibited eosinophil shape changes in dose dependent manners with sub-nanomolar potencies (Fig. 5A and B). IC_{50} values against metabolites were comparable and ranged between 0.1 and 0.9 nM for PGD_2 and six metabolites (Table 3). Eosinophil shape changes induced by 15-deoxy-$\Delta^{12,14}$-PGJ_2 could be inhibited by fevipiprant, however, the dose–response was not sigmoidal.

Similar to eosinophil activation, ILC2 migration (Fig. 5C and D) and cytokine secretion (Fig. 5E–H) could be inhibited by fevipiprant in a concentration dependent manner. In comparison to eosinophils, ILC2 related IC_{50} values were approximately one order of magnitude higher. Migration IC_{50} values ranged between 1.9 and 10.9 nM, IL-5 IC_{50} values ranged between 2.3 and 6.5 nM, and IL-13 IC_{50} values ranged between 2.6 and 8.5 nM (Table 3). 9a,11b-PGF_2 induced cytokine secretion results were highly variable among donors and IC_{50} values could not be determined.

Discussion

In vivo and in vitro, PGD_2 is rapidly degraded to various metabolites which presumably contribute to DP_2 immune cell activation in large part due to their DP_2 selectivity [15, 38]. Here, we show for the first time that ILC2s respond to PGD_2 metabolites by migration and IL-5 and IL-13 secretion. We determined respective EC_{50} values, quantified cellular responses of eosinophils and ILC2s and compared the activation maximal responses with respective PGD_2 responses. DP_2 dependency was demonstrated using fevipiprant which abolished cell activities with nanomolar potencies.

The influence of prostaglandin metabolites on eosinophil cell activation and shape change is well known. Sandig et al. first reported EC_{50} values, which we could largely confirm [19]. EC_{50} concentrations resulted in different rank orders of potencies compared to ours, however, those differences were negligibly small. The potency of 9α,11β-PGF_2 was clearly reduced in both studies compared to other metabolites. Since 9α,11β-PGF_2 has an approximately 130 fold reduced binding affinity to DP_2 compared to PGD_2 [38], it can be assumed that the concentrations used were too low to sufficiently induce a shape changes in eosinophils. Merely concentrations of

(See figure on next page.)

Fig. 3 **A** ILC2 migration in the presence of ascending concentrations of PGD_2 and selected metabolites, n = 3. Values are given as mean ± SD. Nonlinear curve fit with constraints of bottom constant equal to zero and top constant equal to 100 was applied to derive EC_{50} and EC_{70}. **B** Maximal cell migration of PGD_2 and selected metabolites. Absolute numbers of migrated cells were compared and normalized to 100% PGD_2, n = 7. Values are given as mean ± SD. DK-PGD_2: ns, Δ^{12}-PGD_2: ns, 15-deoxy-$\Delta^{12,14}$-PGD_2: p = 0.05, 9α,11β-PGF_2: ns, PGJ_2: ns, Δ^{12}-PGJ_2: p = 0.03 and 15-deoxy-$\Delta^{12,14}$-PGJ_2: p = 0.01. *p < 0.05

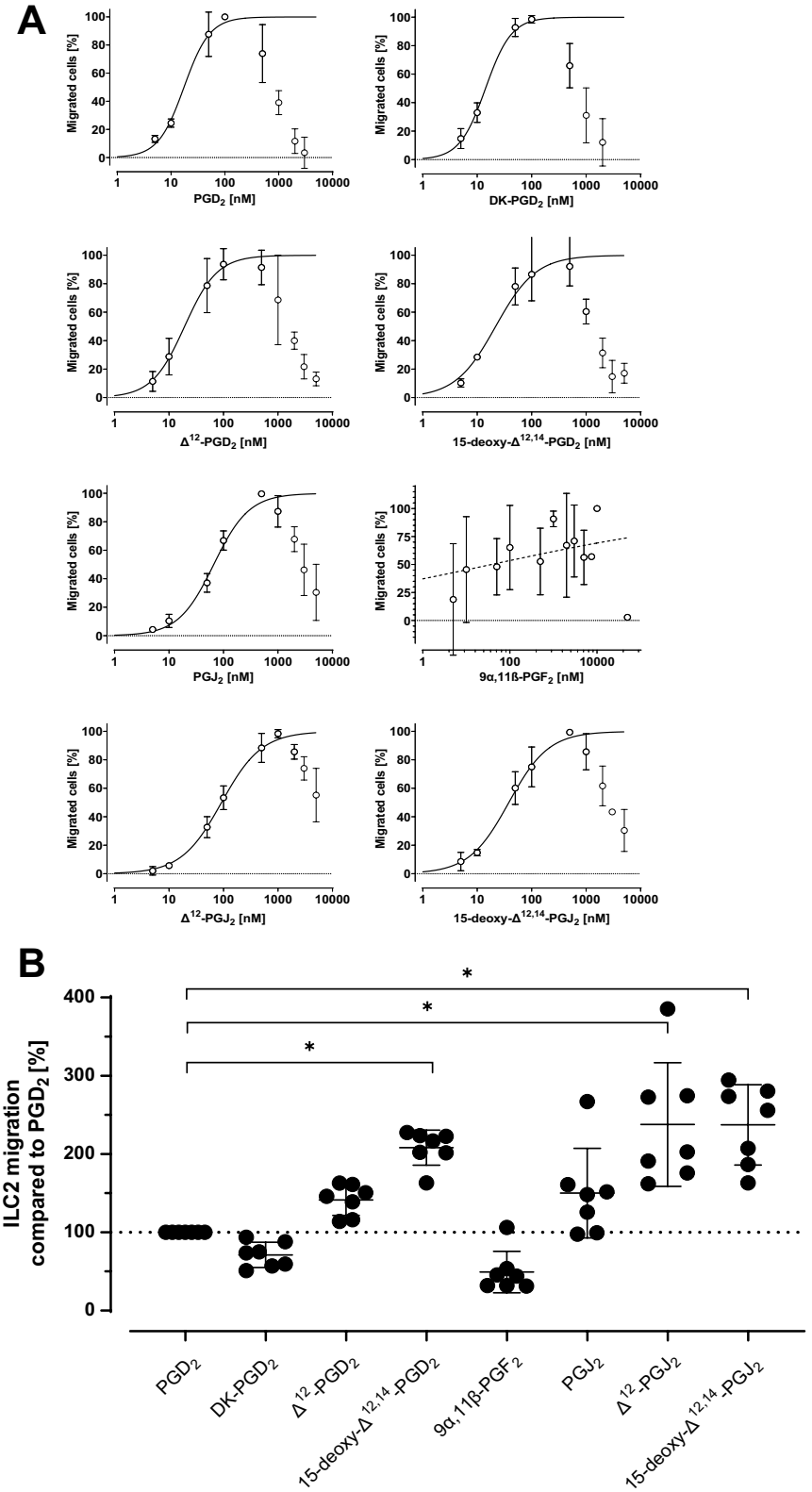

Fig. 3 (See legend on previous page.)

Table 2 EC_{50} values of PG-induced ILC2 migration and IL-5 and IL-13 cytokine secretion were calculated and are given as mean ± standard error of the mean (SEM), n = 3

ILC2 migration and cytokine secretion EC_{50} [nM]			
Metabolite	**Migration**	**IL-5 secretion**	**IL-13 secretion**
PGD_2	17.4 ± 3.9	139.2 ± 15.5	131.9 ± 10.8
DK-PGD_2	14.2 ± 3.4	146.0 ± 18.0	159.2 ± 28.8
Δ^{12}-PGD_2	19.3 ± 3.2	108.1 ± 11.8	125.2 ± 8.3
15-deoxy-$\Delta^{12,14}$-PGD_2	21.8 ± 6.3	175.4 ± 26.4	159.1 ± 13.9
9α,11β-PGF_2	–[a]	526.9 ± 12,926.7	788.3 ± 173.7
PGJ_2	66.3 ± 7.0	244.4 ± 26.3	321.9 ± 43.8
Δ^{12}-PGJ_2	91.7 ± 9.2	234.1 ± 30.6	343.2 ± 52.4
15-deoxy-$\Delta^{12,14}$-PGJ_2	38.1 ± 5.4	185.3 ± 21.5	226.2 ± 35.2

[a] Curve fit was ambiguous, EC_{50} value could not be determined

1 µM demonstrated a shift in FCS properties (Additional file 1: Fig. S1). Comparing the maximal changes in the forward scatters indicated that all metabolites induced shape changes with similar maximal responses. This may imply their comparable agonistic function on eosinophil activation. This finding could be supported by further eosinophil activation data addressing e.g. cell surface CD11b expression or degranulation.

The selective relevance of DP_2 for eosinophil activation has been reported for PGD_2 and DK-PGD_2 using various DP_2 antagonists [19, 39, 40]. Nevertheless, blocking the activation of other metabolites was described only using the dual DP_2 and thromboxane receptor (TP) antagonist ramatroban [19]. We complemented data affirming that metabolites induced eosinophil shape changes via DP_2 selectively using fevipiprant [41].

Less is known about the role of PGD_2 metabolites on ILC2 activation. Recently it was shown that ILC2s produce endogenous PGD_2 upon alarmin activation which was metabolized to PGJ_2, Δ^{12}-PGJ_2, DK-PGD_2 and 15-deoxy-$\Delta^{12,14}$-PGJ_2 in culture supernatants [28]. However, so far only exogeneous and endogeneous PGD_2 was reported to induce migration and IL-5 and IL-13 secretion in ILC2s [26–28]. Here, we show that ILC2s also migrate and release Type 2 cytokines in presence of DK-PGD_2, PGJ_2, Δ^{12}-PGJ_2, Δ^{12}-PGD_2, 15-deoxy-$\Delta^{12,14}$-PGJ_2, and 15-deoxy-$\Delta^{12,14}$-PGD_2. D-series metabolites were more potent than those of the J-series. 9α,11β-PGF_2 was not able to induce ILC2 migration in the concentration range used. The comparably low binding affinity of 9α,11β-PGF_2 to DP_2 might have resulted in the low response. Varying activating potencies among the other metabolites might be related to differences in respective DP_2 binding affinities as well [15, 38], however, EC_{50} rank orders of shape change, migration and cytokine release experiments were different. Moreover, quantifying the maximal assay responses among metabolites revealed that ILC2 cell migration was enhanced in presence of most metabolites compared to PGD_2 while cytokine production was not enhanced. Interestingly, cell migration was strongest for the J-series metabolites Δ^{12}-PGJ_2, 15-deoxy-$\Delta^{12,14}$-PGJ_2 and cytokine secretion was strongest for the D-series metabolites Δ^{12}-PGD_2, 15-deoxy-$\Delta^{12,14}$-PGD_2. Our data may indicate that PGD_2 metabolites contribute predominantly to ILC2 migration rather than cytokine secretion which needs to be confirmed in vivo. Although it is known that numbers of eosinophils and ILC2s are elevated in the airways of severe asthmatic patients [24] little is known about local distributions of PGD_2 metabolite concentrations in human tissues. ILC2 numbers and PGD_2 concentrations in the bronchoalveolar lavage (BAL) fluid were reported to correlate after allergen challenge of mild asthmatics [25]. Moreover, metabolic products of PGD_2 were found in human serum [42], plasma, BAL [43] and urine [44, 45] samples, however, their contribution to the asthmatic disease is poorly understood [20]. Studies on eosinophils in mice showed that Δ^{12}-PGJ_2 mobilizes eosinophils from the bone marrow and facilitates cell extravasation [18] which fits with the observation that PGD_2 is preferably converted to Δ^{12}-PGD_2 and Δ^{12}-PGJ_2 in blood plasma [12]. The contribution of metabolites to cell recruitment might be of biological relevance but remains speculative without further experiments. 9α,11β-PGF_2 is another major degradation products found in human and showed low agonistic potency on eosinophils and ILC2s [42, 44, 46]. At micromolar concentrations, 9α,11β-PGF_2 was able to activate cells, which probably do not represent physiological concentrations of the metabolite. Further, quantification of ILC2 responses indicated a reduced maximal response compared to PGD_2. Therefore, it seems more likely that 9α,11β-PGF_2 does not contribute to DP_2 signaling in vivo but rather serves as an signal-inactivating degradation product.

Blocking with fevipiprant confirmed the DP_2 dependency of ILC2 activities which were comparable to previous experiments performed with PGD_2 [26]. Inhibition of

(See figure on next page.)

Fig. 4 **A** IL-5 (white circles) and IL-13 (black squares) cytokine secretion of ILC2s in the presence of ascending concentrations of PGD_2 and selected metabolites, n = 3. Values are given as mean ± SD. Nonlinear curve fit with constraints of bottom constant equal to zero and top constant equal to 100 was applied to derive EC_{50} and EC_{70}. **B** Maximal cytokine secretion of selected metabolites compared to PGD_2. The absolute concentrations of secreted cytokines were compared and normalized to 100% PGD_2, n = 6. Values are given as mean ± SD. 9α,11β-PGF_2: IL-5 p = 0.006, IL-13 p = 0.02, PGJ_2: IL-5 p = 0.03, IL-13 p = 0.007. *p < 0.05, **p < 0.01, ***p < 0.001, ****p < 0.0001

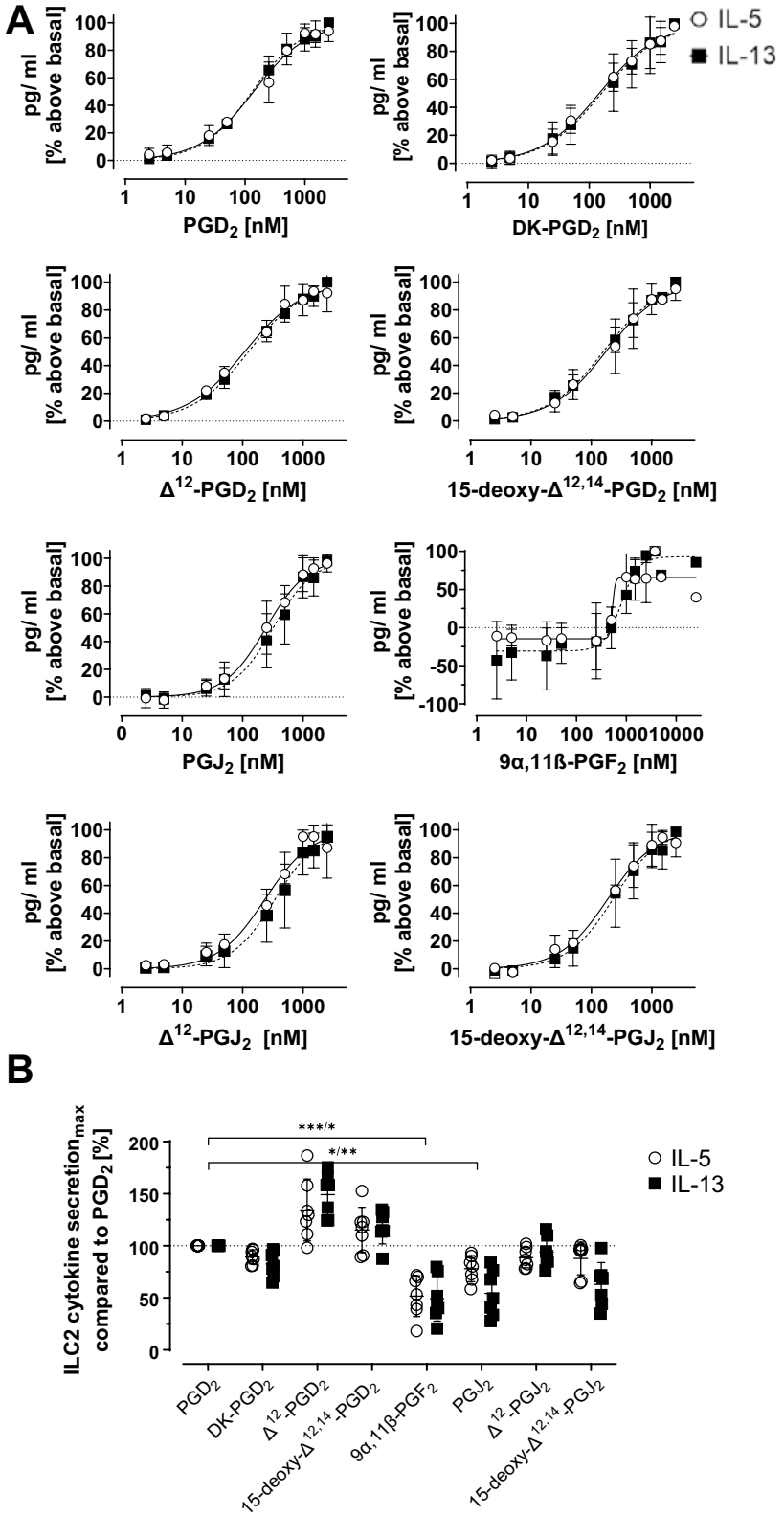

Fig. 4 (See legend on previous page.)

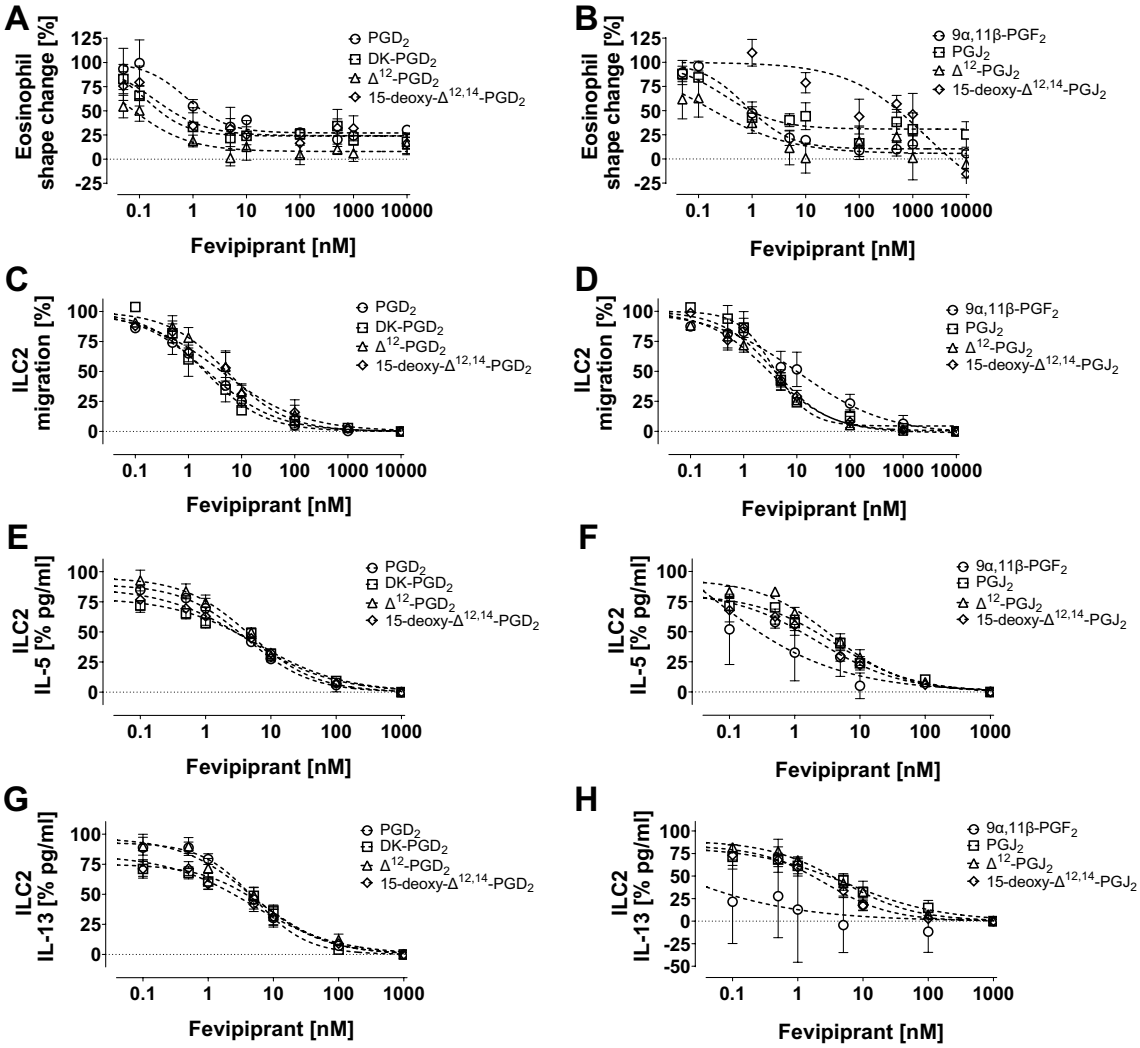

Fig. 5 Inhibition of PGD_2 and metabolite-induced cell activation with DP_2 inhibitor fevipiprant. Cells were incubated with ascending concentrations of fevipiprant and stimulated with EC_{70} concentrations of PGD_2, DK-PGD_2, Δ^{12}-PGD_2, 15-deoxy-$\Delta^{12,14}$-PGD_2, PGJ_2, 9a,11b-PGF_2, Δ^{12}-PGJ_2 and 15-deoxy-$\Delta^{12,14}$-PGJ_2, respectively. **A**, **B** Inhibition of eosinophil shape change, n = 3–5. Top constraints equal 100. **C**, **D** Inhibition of ILC2 migration, n = 4. Top constraints equal 100. **E**, **F** Inhibition of ILC2 IL-5 secretion, n = 4. Bottom constraints equal zero. (G,H) Inhibition of ILC2 IL-13 secretion, n = 4. Bottom constraints equal zero. Values are given as mean ± SEM

Table 3 IC_{50} values of fevipiprant-inhibited eosinophil shape change, ILC2 migration and IL-5 and IL-13 cytokine secretion of ILC2s

IC_{50} fevipiprant [nM]				
Metabolite	**shape change (n = 3–5)**	**Migration (n = 4)**	**IL-5 (n = 4)**	**IL-13 (n = 4)**
PGD_2	0.9 ± 0.2	2.4 ± 0.6	4.2 ± 0.8	5.1 ± 1.1
DK-PGD_2	0.1 ± 0.0	1.9 ± 0.7	6.5 ± 1.6	8.5 ± 2.1
Δ^{12}-PGD_2	0.1 ± 0.0	4.9 ± 1.3	4.8 ± 1.2	4.8 ± 1.3
15-deoxy-$\Delta^{12,14}$-PGD_2	0.5 ± 0.3	4.6 ± 2.0	4.5 ± 1.7	4.6 ± 1.4
9α,11β-PGF_2	0.9 ± 0.1	10.9 ± 7.8	–[a]	–[a]
PGJ_2	0.5 ± 0.2	3.7 ± 0.6	4.0 ± 1.0	5.9 ± 3.6
Δ^{12}-PGJ_2	0.6 ± 0.3	3.1 ± 0.5	3.7 ± 0.9	4.6 ± 1.6
15-deoxy-$\Delta^{12,14}$-PGJ_2	–[a]	3.8 ± 0.8	2.3 ± 0.9	2.6 ± 0.9

Values were calculated from 3 to 5 experiments and are given as mean ± standard error of the mean (SEM)

[a] Curve fit was ambiguous, IC_{50} values could not be determined

15-deoxy-$\Delta^{12,14}$-PGJ_2 activation in eosinophils followed a non-sigmoidal dose–response principle which should be assessed more closely in future studies. Inhibiting PGD_2 signaling has been studied in a wide range of clinical studies due to its key role in allergic inflammation. While fevipiprant itself is no longer being developed for asthma, our findings may be of relevance to other DP_2 antagonists which remain under clinical investigation [22, 47].

Conclusion

PGD_2 metabolites are effective DP_2 agonists and promote eosinophil shape change, ILC2 cell migration and Type 2 cytokine secretion in vitro. They might contribute to ILC2 recruitment in vivo since predominantly ILC2 migration but not ILC2 cytokine secretion or eosinophil shape change was enhanced compared to PGD_2.

Abbreviations

BAL: Bronchoalveolar lavage; BMI: Body mass index; BSA: Bovine serum albumin; CD: Cluster of differentiation; Conc.: Concentration; CRTH2: Chemoattractant receptor-homologous molecule expressed on Th2 cells; DK-PGD_2: 13,14-Dihydro-15-keto-prostaglandin D_2; DMSO: Dimethylsulfoxide; DP: D-prostanoid receptor; DPBS: Dulbecco's Phosphate Buffered Saline; EC_{50}: Half maximal effective concentration; EDTA: Ethylenediaminetetraacetic acid; FSC: Forward scatter; HEPES: 4-(2-Hydroxyethyl)-1-piperazineethanesulfonic acid; IC_{50}: Half maximal inhibitory concentration; IL: Interleukin; ILC2: Type 2 innate lymphoid cells; MFI: Mean fluorescence intensity; PG: Prostaglandin; PHA-M: Phytohemagglutinin-M; SD: Standard deviation; SEM: Standard error of mean; SSC: Sideward scatter.

Supplementary Information

The online version contains supplementary material available at https://doi.org/10.1186/s12931-021-01852-3.

Additional file 1: Table S1. Detailed information on flow cytometric antibodies used for cell sorting of ILC2s. **Table S2.** Calculated agonist EC70 values for PGD2 and seven selected PGD2 metabolites. **Table S3.** Characteristics of study subjects. All subjects had a history of allergic asthma since at least 12 months. BMI had to be between 19 to 32 kg/m2. **Figure S1.** Eosinophil shape change induced by PGD2, DK-PGD2, Δ12-PGD2, 15-deoxy-Δ12,14-PGD2, PGJ2, 9a,11b-PGF2, Δ12-PGJ2 and 15-deoxy-Δ12,14-PGJ2. Granulocytes were isolated from whole blood of asthmatic patients and were incubated with increasing concentrations of metabolites, n=3, 9α,11β-PGF2: n=2. The mean fluorescence values of the forward scatter were determined by flow cytometry and the percentage of shape change above basal was calculated. Values are given as mean ± SD. **Figure S2.** Concentration of IL-5 cytokine secretion of ILC2s in the presence of ascending concentrations of PGD2 and selected metabolites, n=3. Values are given for three different subjects (circle, square and triangle). **Figure S3.** Concentration of IL-13 cytokine secretion of ILC2s in the presence of ascending concentrations of PGD2 and selected metabolites, n=3. Values are given for three different subjects (circle, square and triangle).

Acknowledgements

The authors would like to thank Professor Luzheng Xue (University of Oxford) for his support and help as well as the clinical staff of Fraunhofer ITEM for subject recruitment.

Authors' contributions

All authors added and revised the manuscript. SC: Data curation, formal analysis, methodology, visualization, writing original draft, writing review and editing; CG: Data curation, formal analysis, methodology, visualization, writing review and editing; VJE: Conceptualization, project administration, writing review and editing; SDK: Conceptualization, project administration, writing review and editing; JMH: Conceptualization, writing review and editing; DAS: Conceptualization, project administration, writing review and editing; MM: Conceptualization, writing review and editing. All authors read and approved the final manuscript.

Funding

Open Access funding enabled and organized by Projekt DEAL. This research was supported by Novartis Pharma AG and was performed under a collaboration agreement between Novartis and Fraunhofer ITEM.

Availability of data and materials

The datasets supporting the conclusion of this article are available on reasonable request from MM and DAS.

Declarations

Ethics approval and consent to participate

The study was approved by the Ethics Committee of the Hannover Medical School (7882_BO_S_2018). All subjects gave written informed consent.

Consent for publication

Not applicable.

Competing interests

SC's, CG's, JMH's and MM's institution received funding from ALK, Allergopharma, Astellas, AstraZeneca, GlaxoSmithKline, Janssen Pharmaceutica NV, LETI, Novartis, and Sanofi-Aventis for clinical trial conduct outside the submitted work. JMH reports personal fees from Boehringer Ingelheim, CSL Behring, HAL, Merck, and Novartis for consultancy and lectures outside the submitted work. VJE and SK were employees of Novartis at the time of the study. DAS is an employee of Novartis.

Author details

[1]Department of Biomarker Analysis and Development, Clinical Airway Research, Fraunhofer Institute of Toxicology and Experimental Medicine, Hannover, Germany. [2]Novartis Pharma AG, Basel, Switzerland. [3]Novartis Institutes for Biomedical Research, Cambridge, MA, USA. [4]German Center for Lung Research (BREATH), Hannover, Germany. [5]Department of Respiratory Medicine, Hannover Medical School, Hannover, Germany.

Received: 31 May 2021 Accepted: 27 September 2021
Published online: 07 October 2021

References

1. Kupczyk M, Kuna P. Targeting the PGD2/CRTH2/DP1 signaling pathway in asthma and allergic disease current status and future perspectives. Drugs. 2017;77:1281–94. https://doi.org/10.1007/s40265-017-0777-2.
2. Balzar S, et al. Mast cell phenotype, location, and activation in severe asthma. Data from the Severe Asthma Research Program. Am J Respir Crit Care Med. 2011;183:299–309. https://doi.org/10.1164/rccm.201002-0295OC.
3. Domingo C, Palomares O, Sandham DA, Erpenbeck VJ, Altman P. The prostaglandin D2 receptor 2 pathway in asthma a key player in airway inflammation. Respir Res. 2018;19:189.
4. García-Solaesa V, et al. The prostaglandin D2 receptor (PTGDR) gene in asthma and allergic diseases. Allergol Immunopathol. 2014;42:64–8. https://doi.org/10.1016/j.aller.2012.12.002.
5. Kostenis E, Ulven T. Emerging roles of DP and CRTH2 in allergic inflammation. Trends Mol Med. 2006;12:148–58. https://doi.org/10.1016/j.molmed.2006.02.005.

6. Hirai H, et al. Prostaglandin D2 selectively induces chemotaxis in T helper type 2 cells, eosinophils and basophils via seven-transmembrane receptor CRTH2. J Exp Med. 2001;193:255–61.
7. Monneret G, Gravel S, Diamond M, Rokach J, Powell WS. Prostaglandin D2 is a potent chemoattractant for human eosinophils that acts via a novel DP receptor. Blood. 2001;98:1942–8.
8. Mjösberg JM, et al. Human IL-25- and IL-33-responsive type 2 innate lymphoid cells are defined by expression of CRTH2 and CD161. Nat Immunol. 2011;12:1055–62. https://doi.org/10.1038/ni.2104.
9. Gervais FG, et al. Selective modulation of chemokinesis, degranulation, and apoptosis in eosinophils through the PGD2 receptors CRTH2 and DP. J Allergy Clin Immunol. 2001;108:982–8. https://doi.org/10.1067/mai.2001.119919.
10. Stubbs VEL, et al. Indomethacin causes prostaglandin D(2)-like and eotaxin-like selective responses in eosinophils and basophils. J Biol Chem. 2002;277:26012–20. https://doi.org/10.1074/jbc.M201803200.
11. Peinhaupt M, Sturm EM, Heinemann A. Prostaglandins and their receptors in eosinophil function and as therapeutic targets. Front Med. 2017. https://doi.org/10.3389/fmed.2017.00104.
12. Schuligoi R, et al. PGD_2 metabolism in plasma: kinetics and relationship with bioactivity on DP1 and CRTH2 receptors. Biochem Pharmacol. 2007;74:107–17. https://doi.org/10.1016/j.bcp.2007.03.023.
13. Suzuki F, Hayashi H, Hayashi O. Transport of prostaglandin D_2 into brain. Brain Res. 1986;385:321–8.
14. Giles H, Leff P. The biology and pharmacology of PGD2. Prostaglandins. 1988;35:277–300.
15. Gazi L, et al. Δ^{12}-prostaglandin D_2 is a potent and selective CRTH2 receptor agonist and causes activation of human eosinophils and Th2 lymphocytes. Prostaglandins Other Lipid Mediat. 2005;75:153–67. https://doi.org/10.1016/j.prostaglandins.2004.11.003.
16. Pettipher R, Hansel TT, Armer R. Antagonism of the prostaglandin D2 receptors DP1 and CRTH2 as an approach to treat allergic diseases. Nat Rev. 2007;6:313–25. https://doi.org/10.1038/nrd2266.
17. Fitzpatrick FA, Wynalda MA. Albumin-catalyzed metabolism of prostaglandin D_2. Identification of products formed in vitro. J Biol Chem. 1983;258:11713–8.
18. Heinemann A, Schuligoi R, Sabroe I, Hartnell A, Peskar BA. Delta 12-prostaglandin J2, a plasma metabolite of prostaglandin D2, causes eosinophil mobilization from the bone marrow and primes eosinophils for chemotaxis. J Immunol. 2003;170:4752–8. https://doi.org/10.4049/jimmunol.170.9.4752.
19. Sandig H, Andrew D, Barnes AA, Sabroe I, Pease J. 9α,11β-PGF_2 and its stereoisomer $PGF_{2\alpha}$ are novel agonists of the chemoattractant receptor, CRTH2. FEBS Lett. 2006;580:373–9. https://doi.org/10.1016/j.febslet.2005.11.052.
20. Bochenek G, Nagraba K, Nizankowska E, Szczeklik A. A controlled study of 9α,11β-PGF_2 (a prostaglandin D_2 metabolite) in plasma and urine of patients with bronchial asthma and healthy controls after aspirin challenge. J Allergy Clin Immunol. 2003;111:743–9. https://doi.org/10.1067/mai.2003.1387.
21. Monneret G, Li H, Vasilescu J, Rokach J, Powell WS. 15-Deoxy-$\Delta^{12,14}$-prostaglandins D_2 and J_2 are potent activators of human eosinophils. J Immunol. 2002;168:3563–9. https://doi.org/10.4049/jimmunol.168.7.3563.
22. Singh D, Ravi A, Southworth T. CRTH2 antagonists in asthma: current perspectives. Clin Pharmacol. 2017;9:165–73. https://doi.org/10.2147/CPAA.S119295.
23. Kerstjens HAM, Gosens R. Prostaglandin D2: the end of a story or just the beginning? Lancet Respirat Med. 2020;20:2213–600. https://doi.org/10.1016/S2213-2600(20)30449-5.
24. Smith SG, et al. Increased numbers of activated group 2 innate lymphoid cells in the airways of patients with severe asthma and persistent airway eosinophilia. J Allergy Clin Immunol. 2016;137:75–86. https://doi.org/10.1016/j.jaci.2015.05.037.
25. Winkler C, et al. Activation of group 2 innate lymphoid cells after allergen challenge in asthmatic patients. J Allergy Clin Immunol. 2019;144:61–9. https://doi.org/10.1016/j.jaci.2019.01.027.
26. Hardman C, et al. Fevipiprant, a selective prostaglandin D2 receptor 2 antagonist, inhibits human group 2 innate lymphoid cell aggregation and function. J Allergy Clin Immunol. 2019;143:2326–9. https://doi.org/10.1016/j.jaci.2019.02.016.
27. Xue L, et al. Prostaglandin D2 activates group 2 innate lymphoid cells through chemoattractant receptor-homologous molecule expressed on TH2 cells. J Allergy Clin Immunol. 2014;133:1184–94. https://doi.org/10.1016/j.jaci.2013.10.056.
28. Maric J, et al. Cytokine-induced endogenous production of prostaglandin D2 is essential for human group 2 innate lymphoid cell activation. J Allergy Clin Immunol. 2019;143:2202–14. https://doi.org/10.1016/j.jaci.2018.10.069.
29. Erpenbeck VJ, et al. The oral CRTh2 antagonist QAW039 (fevipiprant): a phase II study in uncontrolled allergic asthma. Pulmonary Pharmacol Therap. 2016;39:54–63. https://doi.org/10.1016/j.pupt.2016.06.005.
30. Bateman ED, et al. Fevipiprant, an oral prostaglandin DP2 receptor (CRTh2) antagonist, in allergic asthma uncontrolled on low-dose inhaled corticosteroids. Eur Respir J. 2017. https://doi.org/10.1183/13993003.00670-2017.
31. Gonem S, et al. Fevipiprant, a prostaglandin D2 receptor 2 antagonist, in patients with persistent eosinophilic asthma a single-centre, randomised, double-blind, parallel-group, placebo-controlled trial. Lancet Respir Med. 2016;4:699–707.
32. Saunders R, et al. DP2 antagonism reduces airway smooth muscle mass in asthma by decreasing eosinophilia and myofibroblast recruitment. Sci Transl Med. 2019. https://doi.org/10.1126/scitranslmed.aao6451.
33. Brightling CE, et al. Effectiveness of fevipiprant in reducing exacerbations in patients with severe asthma (LUSTER-1 and LUSTER-2): two phase 3 randomised controlled trials. Lancet Respir Med. 2020;20:2213–600. https://doi.org/10.1016/S2213-2600(20)30412-4.
34. Castro M, et al. Efficacy and safety of fevipiprant in patients with uncontrolled asthma: two replicate, phase 3, randomised, double-blind, placebo-controlled trials (ZEAL-1 and ZEAL-2). EClinicalMedicine. 2021;35:100847.
35. Sykes DA, et al. Fevipiprant (QAW039), a slowly dissociating CRTh2 antagonist with the potential for improved clinical efficacy. Mol Pharmacol. 2016;89:593–605. https://doi.org/10.1124/mol.115.101832.
36. Xue L, et al. Fevipiprant inhibits DP2 mediated upregulation of tissue remodeling genes and autocrine prostaglandin D2 production in Tc2 cells. Am J Respir Crit Care Med. 2020;201:1.
37. Sabroe I, et al. Differential regulation of eosinophil chemokine signaling via CCR3 and non-CCR3 pathways. J Immunol. 1999;162:2946–55.
38. Sawyer N, et al. Molecular pharmacology of the human prostaglandin D_2 receptor, CRTH2. Br J Pharmacol. 2002;137:1163–72. https://doi.org/10.1038/sj.bjp.0704973.
39. Murphy S, et al. GB001 potently inhibits PGD2 metabolite-induced DP2-mediated cell signaling and eosinophil activation. Eur Respir J. 2020;56:2902.
40. Pettipher R, et al. Pharmacologic profile of OC000459, a potent, selective, and orally active D prostanoid receptor 2 antagonist that inhibits mast cell-dependent activation of T helper 2 lymphocytes and eosinophils. J Pharmacol Exp Therap. 2012;340:473–82. https://doi.org/10.1124/jpet.111.187203.
41. Sandham DA, et al. Discovery of fevipiprant (NVP-QAW039), a potent and selective DP2 receptor antagonist for treatment of asthma. ACS Med Chem Lett. 2017;8:582–6. https://doi.org/10.1021/acsmedchemlett.7b00157.
42. Nassiri M, Eckermann O, Babina M, Edenharter G, Worm M. Serum levels of 9α,11β-PGF_2 and cyseinyl leukotrienes are useful biomarkers for anaphylaxis. J Allergy Clin Immunol. 2016;137:312–4. https://doi.org/10.1016/j.jaci.2015.06.006.
43. Mastalerz L, et al. Induced sputum eicosanoids during aspirin bronchial challenge of asthmatic patients with aspirin hypersensitivity. Allergy. 2014;69:1550–9. https://doi.org/10.1111/all.12512.
44. Liston TE, Roberts LJ. Metabolic fate of radiolabeled prostaglandin D_2 in a normal human male volunteer. J Biol Chem. 1985;260:13172–80.
45. Kolmert J, Dahlén S-E, Wheelock CE. Reply to Thomson: Exposure to active and passive tobacco smoke on urinary eicosanoid metabolites in type 2 asthma. Am J Respir Critic Care Med. 2021;203:1204–5. https://doi.org/10.1164/rccm.202101-0208LE.
46. Liston TE, Jackson Roberts II L. Transformation of prostaglandin D2 to 9α,11β-(15S)-trihydroxyprosta-(5Z, 13E)-dien-1-oic acid (9α,11β-prostaglandin F2): a unique biologically active prostaglandin produced enzymatically in vivo in humans. Proc Natl Acad Sci USA. 1985;82:6030–4.
47. Asano K, et al. A Phase 2a Study of DP2 Antagonist GB001 for Asthma. J Allergy Clin Immunol. 2020;8:1275–83. https://doi.org/10.1016/j.jaip.2019.11.016.

Publisher's Note